applied sciences

MDPI

Article

Effect of Degassing on the Stability and Reversibility of Glycerol/ZSM-5 Zeolite System

Yafei Zhang [1,2], Rui Luo [3], Qulan Zhou [2,*], Xi Chen [4,5,*] and Yihua Dou [1]

1 School of Mechanical Engineering, Xi'an Shiyou University, Xi'an 710065, China; effyzhang@126.com (Y.Z.); yhdou@vip.sina.com (Y.D.)
2 State Key Laboratory of Multiphase Flow in Power Engineering, Xi'an Jiaotong University, Xi'an 710049, China
3 Xi'an Thermal Power Research Institute Co., Ltd., Xi'an 710054, China; luorui@tpri.com.cn
4 Department of Earth and Environmental Engineering, Columbia University, New York, NY 10027, USA
5 International Center for Applied Mechanics, SV Lab, School of Aerospace, Xi'an Jiaotong University, Xi'an 710049, China
* Correspondence: qlzhou@mail.xjtu.edu.cn (Q.Z.); xichen@columbia.edu (X.C.); Tel.: +86-135-7199-5532 (Q.Z.); +86-187-1094-7000 (X.C.)

Received: 6 June 2018; Accepted: 26 June 2018; Published: 29 June 2018

Featured Application: A system composed of liquid and hydrophobic nanoporous materials can perform high energy absorption efficiency when applying external pressure. Such an advanced energy absorption system has the potential application for high-performance protection devices to protect the personnel and civil infrastructures from impact, and other areas that involve energy absorption/conversion. Gaseous phase in a liquid/nanoporous system plays roles during application. Understanding the effect of the amount of residual gas on the liquid/nanoporous system will help to guide the pretreatment of the liquid/nanoporous material mixture before encapsulating.

Abstract: Gaseous phase plays roles in a liquid/nanoporous system during application that adequate attention should be paid to the gaseous effects and the nanoscale gas-liquid interaction. In the present study, two glycerol/ZSM-5 zeolite systems with different amount of residual gas are compared by performing a series of experiments. Influences of loading rate, as well as system temperature on the gas-liquid interactions, are studied. Results show that vacuum degassing pretreatment is required to obtain a reversible and stable energy absorption system. Moreover, the influence of gas on a liquid/nanoporous system is found to mainly act on the liquid outflow. After the routine vacuum degassing pretreatment, the residual air that is left in the nanopores is around 0.9014 nm^{-3} per unit specific pore volume, as presented in the current study. During compression, the existing gas left in the nanochannel tends to gather into the gas cluster, which further promotes the liquid outflow during unloading. However, excessively dissolved gas may reduce the driving force for liquid outflow by breaking the continuity of the liquid molecular chain in nanochannel. Consequently, small bubbles as a labile factor in the system must be excluded for the steady use of the system. This work sheds some light on the effect of the amount of residual gas on the liquid/nanoporous system and gives guidance on the pretreatment of the liquid/nanoporous material mixture before encapsulating.

Keywords: liquid/nanoporous material system; gas amount; degassing pretreatment; liquid outflow; liquid-gas interaction

1. Introduction

When nonwetting liquid is forced into hydrophobic nanopores by applying external pressure, a large amount of mechanical energy can be converted to solid-liquid interfacial energy [1–6]. Due to

the ultra-large solid-liquid interface, the pressure-induced intrusion of liquid into nanopores can contribute to a highly efficient energy absorption system [7,8]. Such advanced energy absorption system has the potential application for high-performance protection devices to protect the personnel and civil infrastructures from impact [9–13].

In comparison with the various types of materials developed for impact protection, the nonwetting liquid-hydrophobic nan-oporous system possesses the advantages of high energy absorption efficiency [14], ultra-fast energy dissipation rate [14], and fully reusability after up to thousands of cyclic loadings. However, not all of the tested nonwetting liquid-hydrophobic nanopores systems are reusable [15]. For a number of porous materials, it has been observed that the confined liquid tends to be "locked" inside the nanopores after intrusion [16,17], and may flow out again after certain irritation, such as lifting the system temperature [18].

For a steady use, the stability of the nonwetting liquid dispersed in the porous material has been studied in a number of works. Q Yu et al. [19] reported a jump phenomenon in a water and hydrophobic zeolites system and introduced a jump avoidance criterion through the frequency response function analysis. VD Borman et al. [20] studied the physical mechanism to describe the formation process of a stable state of nonwetting liquid filling porous material. Watt-Smith MJ et al. [21] constructed models representing the pore structures of amorphous, mesoporous silica pellets, and explained the physical processes of mercury retraction and entrapment in silica materials. Results showed that the portion of liquid confined in porous materials varies with the porosity, the average radius, the width of the pore size distribution, the concentration of substances in water, and the temperature.

To improve the system's reusability, experiments on the behaviors of nanoporous energy absorption systems that were subjected to cyclic loadings and the molecular dynamic simulations on mechanisms of liquid intrusion into nanopores have also been carried out. Adding chemical additives into water/nanopores systems can modify the inner surface of the porous material, change liquid-solid interaction, and improve the system's recoverability by assisting the liquid outflow. Kong et al. [22] found the system recoverability to be strongly dependent on the NaCl concentration. As NaCl concentration increased from 0% to 25.9 wt. %, the recoverability was improved by a factor of 3. Sun et al. [23] reported a defiltration control method of the zeolite ZSM-5/liquid system by adding sodium hydroxide (NaOH). They believed the infiltration of NaOH aqueous solutions would increase the density of silanol (Si-OH) groups on the inner surface of the porous ZSM-5, which helped to convert the originally hydrophobic surface to hydrophilic that ceased the liquid outflow. Lifting the system temperature is beneficial in establishing a recoverable and reusable energy absorption system. Correspondingly, the weakened intermolecular forces and temperature sensitivity of liquid viscosity may contribute to the infiltration and outflow process at a higher temperature level. Kong and Qiao [24] improved the system recoverability significantly by lifting system temperature in a water/hydrophobic mesoporous silica system. Zhang et al. [18] conducted cyclic loading experiment on a glycerol/ZSM-5 zeolite system, indicating that higher system temperature enable to enlarge the entry area of the nanochannels and to trigger the outflow of glycerol molecules. As gas is inevitable in a liquid/nanoporous system, gaseous phase trapped in nanoholes plays an important role in the system's reversibility. In 2007, Qiao et al. [25] reported that the gas-liquid interaction to be an indispensable factor in nanoenvironments. Through a molecular dynamics simulation, they found the gas molecules in relatively large nanochannels would be dissolved in the liquid during pressure-induced infiltration, leading to a so-called phenomenon of "nonoutflow", while gas molecules tended to form clusters in relatively small nanochannels by triggering liquid defiltration at a reduced pressure. Until 2014, Sun et al. [26] reported a series of experimental results on a water/zeolite β system, showing that the gas molecules acted as a dominant factor in affecting the liquid motion, and the gas nanophase's effect on water "outflow" was significantly time-dependent. Nano-confined liquid behavior exhibited unusual characteristics, such as the exceptionally high transport rate when compared with bulk fluid, which could not be explained by conventional continuum theories [27–31].

As gas plays roles in a liquid/nanoporous system during application, adequate attention should be paid to the gas phase effects and the nanoscale gas-liquid interaction. However, to the best of the authors' knowledge, the available researches on this topic are rather limited and the mechanisms of gas-liquid interaction are still unclear.

In this study, a series of comparative experiments are carried out on a degassed glycerol/ZSM-5 zeolite system and a normal glycerol/ZSM-5 zeolite system without degassing pretreatment. Keep in mind that the degassing treatment can only reduce the amount of residual gas in nanopores. In addition, the complete eliminating of gas in nanopores is almost impossible, and hence, two systems with different amount of residual gas are compared. Influences of the loading rate as well as the system temperature on the gas-liquid-solid interactions are studied. Results show that the degassing treatment is necessary to obtain a more reversible and stable energy absorption system.

2. Materials and Methods

2.1. Material Characterization

The ZSM-5 zeolite material was acquired from Shanghai Fuxu Molecular Sieve Limited Company in China. The particle size of the raw material is around 3.5 μm and the Na_2O concentration is 0.046%. To improve the purity of the sample material, the raw material is pretreated in a tube furnace under 873 K for six h. After decontamination pretreating, the properties of the zeolite are characterized by using Quantachrome Autosorb-iQ-MP gas sorption analyzer (Quantachrome Instruments, Boynton Beach, FL, USA). Its specific surface area and pore volume are determined to be 638.01 m^2/g and 510 mm^3/g, respectively. Through a Non-Local Density Functional Theory (DFT) analysis, both micro and meso pores are discovered in the sample. The micropore size is 0.524 nm and the mesopore size is around 2.114 nm. It is believed that the glycerol molecules only intrude into the mesopores (2.114 nm) under the infiltration pressure of 15~20 MPa in the present work, because the infiltration pressure of water molecules into MFI zeolite's micro pores around 0.5 nm are above 100 MPa, according to previous studies [5,32], and the size of glycerol molecule (about 0.62 nm) is larger than the size of water molecule. Although the glycerol molecules cannot intrude in the micropores (0.524 nm), the existence of micropores is of great importance for both infiltration and defiltration processes, especially for gaseous phase that is trapped in micropores, which cannot be neglected. So, the most probable pore size of mesopore (2.114 nm), the total surface area (638.01 m^2/g), and pore volume (510 mm^3/g) should be used for the calculation of relative parameters.

2.2. Sample Preparation

1.0 g of pretreated zeolite is suspended in 10 mL pure glycerol, forming a milklike liquid. Two conditions of glycerol/ZSM-5 zeolite systems are prepared with different amount of initial residual gas in the system. One condition, called the undegassed condition, is obtained by immersing zeolite into glycerol, and the mixture is placed in a dessicator for 12 h. The other condition, which is called degassed condition, is obtained by placing the glycerol/zeolite mixture in vacuum (0.003 MPa) for 12 h, so as to remove excessive air bubbles. Note that the degassing pretreatment could not eliminate gaseous phase completely, while there are still residual gas in nanopores. Degassing operation only changes the amount of gas that is left in nanopores when compared to the undegassed condition.

The after pretreated mixture is further sealed in a testing chamber, as illustrated in Figure 1. The volume of the chamber is 10 mL. The pressure could be applied by the piston with a diameter of 14 mm. The pressure holding ability of the chamber under different system temperatures is verified by keeping the pressure at the maximum for 600 s, with negligible pressure drop. Reference compression test of pure glycerol is carried out prior to testing any specific mixture. The difference between the mixture and reference is used to obtain the sorption isotherm.

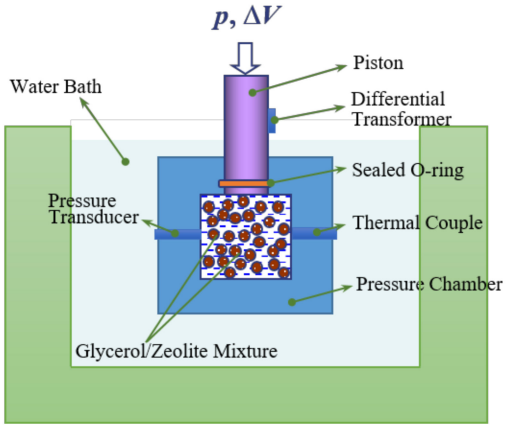

Figure 1. Schematic of experimental set-up.

2.3. Setup and Procedures of the Energy Absorption Experiment

A series of pressure-induced infiltration tests are conducted on a glycerol/ZSM-5 zeolite system. The schematic sketch of the experimental set-up is shown in Figure 1. The pressure-volume controlled testing chamber is a hexahedron cavity that is made of 1Cr13 stainless steel. In order to eliminate air bubbles during the sample filing procedure, the inner surfaces of the chamber are finely filleted. A polished steel piston is assembled in the center of the chamber's upper face, tightly sealed by an O-ring. The piston can be compressed into the chamber at various loading rates (0.01–0.1 mm/s) using a servo motor. Pressure in the chamber can be adjusted in the range of 0 to 60 MPa. The pressure chamber is immersed in a large electric-heated thermostatic water bath (from room temperature to 368 K) to gain control of the system temperature during test. A pressure transducer and a type-E thermal couple are attached to the front and back sides of the chamber to acquire the temperature and pressure of the system. A linear voltage differential transformer is attached on the piston to record its displacement. The real time pressure, temperature, and displacement signals are analyzed by an NI LabVIEW data acquisition system.

During experiment, the piston is moved downwards at a constant velocity in order to impose pressure on the mixture inside the chamber. Once the pressure reached the desired value, given as 50 MPa in this test, the piston starts to retract at the same rate. Under each working condition, the sample is compressed with ten successive loading-unloading cycles for a better observation on the system's stability and reversibility performances. P-ΔV curves (pressure-specific volume change curves) inside the pressure chamber are obtained to analyze the performance of the glycerol/zeolite system. P, which is defined as the pressure of the system, can be directly obtained from the pressure transducer. The specific volume change ΔV is defined as the volume change of the system per unit mass of zeolite and it equals the volume occupied by piston $A \times \Delta d$, where A and Δd is the cross-sectional area and displacement of the piston, respectively.

3. Results

The surface treated zeolite is lyophobic to glycerol, and thus an external pressure is required to induce the intrusion of glycerol molecules into the nanopores. When the external pressure retracts, the amount of glycerol molecules flowing out of the nanochanel is closely related to the state of gaseous phase in the system. In current study, two systems with different amount of residual gas are investigated, while the residual gas in nanopores after degassing pretreatment is estimated via test. Then, cyclic loading/unloading experiments are carried out on undegassed and degassed glycerol/zeolite systems under loading rate of 0.01 mm/s and 0.10 mm/s, with different system temperatures of 303 K and 348 K, respectively. Effects of the gas amount, the loading rate,

and the system temperature are studied, and the mechanisms of gaseous phase on liquid outflow are also illuminated.

3.1. Residual Gas in Nanopores of Undegassed and Degassed Mixture

Figure 2 are photos of glycerol/zeolite mixture taken after different treatment conditions, which show the gas content of the system before and after degassing treatment. Figure 2a is taken after glycerol/zeolite mixture placing at room temperature in a drying condition for 12 h, which demonstrates the gas content of an undegassed system. It is seen that there are a great amount of air bubbles suspended in the mixture. These small bubbles cannot surface because of the viscosity resistance of the liquid. Figure 2b is taken after placing the glycerol/zeolite mixture in vacuum for 12 h, representing the gas content of a degassed system. After 12 h' vacuum degassing, there are no visible bubbles in the system. However, we still carry out a more strict residual air test to estimate the amount of air that stayed in the zeolite's nanopores for degassed mixtures. The following paragraphs are the detailed procedural and analysis of the residual air test of the degassed system. Figure 2c is taken after the residual air test. The bubbles on the surface of the mixture prove that the used degassing treatment under normal temperature cannot eliminate air in nanopores completely.

(a) undegassed mixture (**b**) degassed mixture (**c**) degassed mixture after heating in vacuum

Figure 2. Photos of glycerol/zeolite mixture taken after different treatment.

The residual air test is conducted with a DZF-6000 vacuum drying oven (Xi'an Yu Hui Experimental Apparatus, Xi'an, China). Put the degassed mixture in the vacuum drying oven, and vacuumize the oven to the maximum vacuum degree (0.003 MPa). Then, start the heating schedule of the oven to elevate the inside temperature. With the increase of temperature, the residual air in zeolite will get out of the porous channel gradually; meanwhile, the changing temperature and the pressure of the vacuum drying oven are recorded. Thus, the amount of air that is released from nanopores under certain temperatures can be calculated through the ideal gas law.

The real gas can be considered as ideal gas when both molecular size and inter molecular attractions could be neglected. The test temperature is from 303.15 to 373.15 K and the test pressure is from approximate vacuum to atmosphere. For a large volume at lower pressures, because the average distance between adjacent molecules becomes much larger than the molecular size, the neglect of molecular size becomes less important for lower densities. On the other side, with increasing temperatures, the relative importance of intermolecular attractions diminishes with increasing thermal kinetic energy. Therefore, the ideal gas law can be applied.

Since the absolute vacuum is unavailable, there is still air left in the oven at the highest vacuum degree. In addition, the vacuum drying oven may leak during heating process. A reference test with the same volume of pure glycerol is carried out. For both reference test and test with the degassed mixture, the temperature inside the oven is set to increase from 303.15 to 373.15 K, and the pressure

variation is recorded during heating. Both pure glycerol and glycerol/zeolite mixture are vacuum degassing pretreated before test.

For reference test, there is:

$$pV_0 = n_0RT \tag{1}$$

where, p is the absolute pressure inside the vacuum drying oven, V_0 is the volume of the vacuum drying oven, which is a constant and can be measured in advance, n_0 is the moles of air released during reference test, R is the ideal gas constant, and T is the temperature inside the vacuum drying oven.

For test with glycerol/zeolite mixture, there is:

$$pV_0 = (n_0 + \Delta n)RT \tag{2}$$

where, Δn is the amount of air released from nanopores under a certain temperature.

The n-T curve of reference test and test with degassed glycerol/zeolite mixture is graphed in Figure 3.

From Figure 3, it is clearly observed that there is 4.642×10^{-4} mol·g^{-1} air released from nanopores under 373.15 K. As the specific pore volume for pristine zeolite is about 0.31 cm^3·g^{-1}, there are at least 0.9014 nm^{-3} per unit specific pore volume air still in zeolite after vacuum degassing pretreatment.

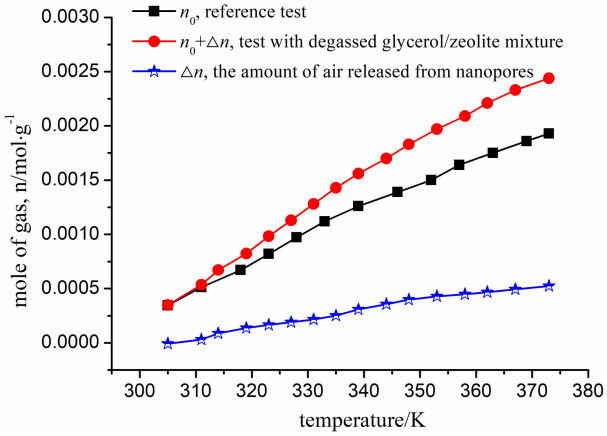

Figure 3. The amount of air released from nanopores with the increase of temperature after degassing pretreatment.

It is with regret that the above method is not suitable for estimating residual air in the undegassed system, since the amount of gas during vacuumizing at the very beginning cannot be quantified.

3.2. Effect of Gas Amount under Different Loading Rates and System Temperatures

3.2.1. P-ΔV Curves of Energy Absorption Experiment

Figure 4 shows the P-ΔV curves (pressure-specific volume change curves) of both undegassed and degassed glycerol/zeolite systems under static/fast loading rate and at the room/lifted system temperature. At the beginning of loading, glycerol stayed outside the hydrophobic nanopores at relative lower pressure. P changes linearly with ΔV in this stage. Once the pressure rises beyond the critical infiltration pressure, the glycerol molecules overcomes the capillary resistance and flows into the nanopores, forming an infiltration plateau. When the nanopores are filled, the system compressibility featured the linear compression behavior of liquid filled solid phase. During the unloading process, glycerol molecules flow out of the nanopores until the pressure is below a critical defiltration pressure. When the external pressure is reduced back to 0.1 MPa, the isotherm curve does not completely return to its origin. Different degrees of outflow of the invaded glycerol molecules perform under different working conditions.

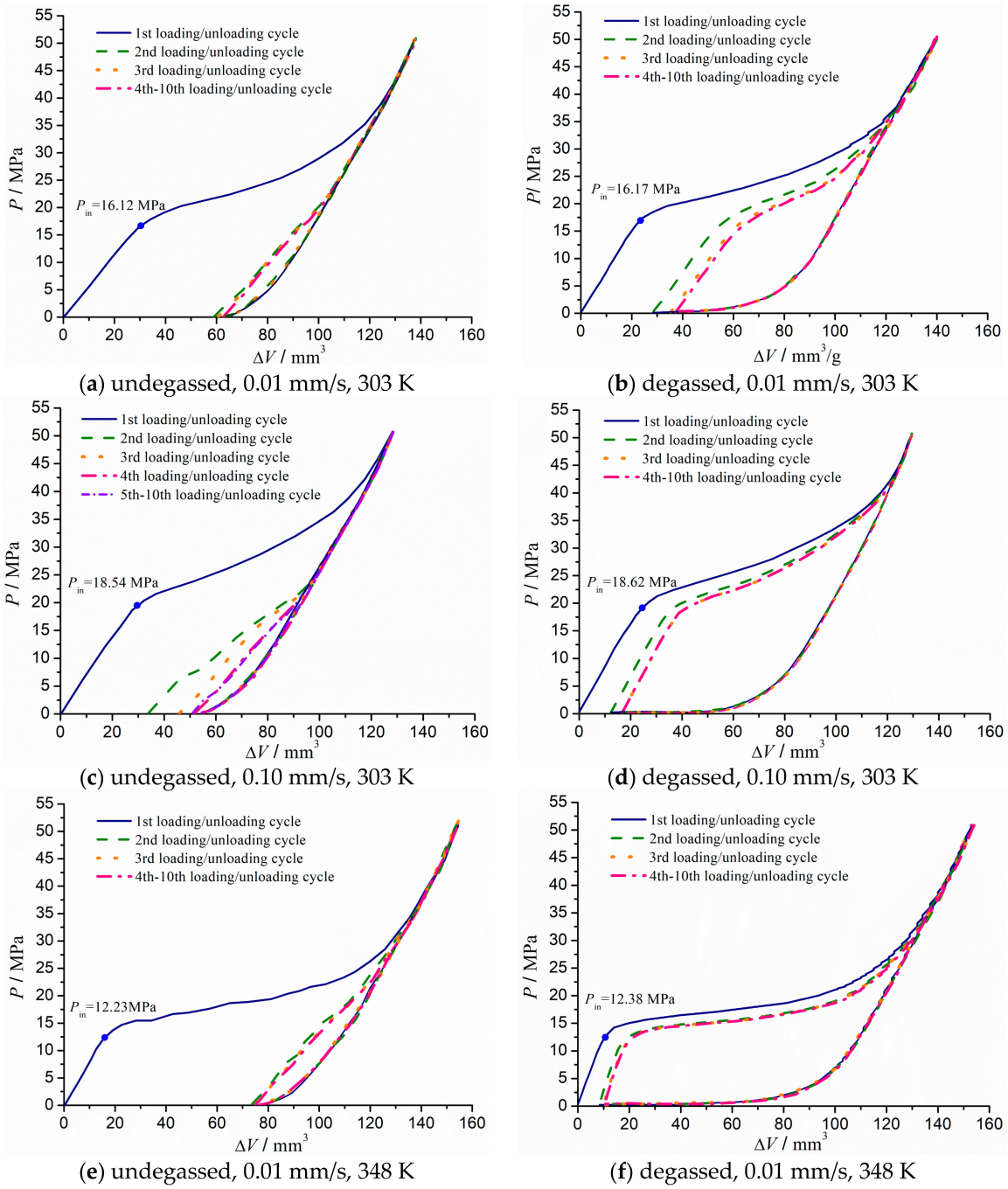

Figure 4. *P*-Δ*V* curves of undegassed and degassed glycerol/zeolite system under ten cyclic loadings (loading rate 0.01 mm/s and 0.10 mm/s; system temperature 303 K and 348 K).

3.2.2. Comparison of *P*-Δ*V* Curves in Comparative Working Condition

Figure 4a,c show the 10 cycles of *P*-Δ*V* curves of the undegassed glycerol/zeolite system at 0.01 mm/s and 0.10 mm/s, respectively. At both loading rates, the glycerol/zeolite system without degassing pretreatment acts as a disposable system. After the 1st intrusion, a large amount of accessible nanopore space is permanently occupied by the invaded glycerol molecules, thus little infiltration is allowed in subsequent cycles. In Figure 4c, although a higher loading rate leads a better outflow after the first intrusion, the hysteresis loop of the undegassed system shrinks afterwards.

Figure 4b and d show the 10 cycles of P-ΔV curves of the degassed glycerol/zeolite system at 0.01 mm/s and 0.10 mm/s separately. When comparing with the undegassed condition, eliminating excessive air bubbles during preparing glycerol/zeolite mixture promotes the reversibility of the system dramatically. In the degassed system, although part of the glycerol molecules trapped in the nanopores and could not flow out of the channels freely after the first cycle, the system reaches its thorough balance, and performs a pressure plateau after the first two or three cycles.

Furthermore, the P-ΔV curves of the degassed and the undegassed systems at a lifted system temperature of 348 K are obtained. The results are plotted in Figure 4e,f. As shown in Figure 4f, the stability of the degassed system is still good at higher system temperature, and the reversibility of the degassed system is improved as well. The system achieves its throughput balance after three cycles. While for an undegassed system in Figure 4e, the P-ΔV curves during loading processes fluctuate, indicating an unstable intrusion process. This is caused by the enhanced solubility of gaseous phase under higher system temperature. The detailed liquid-gas interaction will be analyzed in Section 4, the discussion section.

3.2.3. Effect of Gas Amount on Liquid Outflow

Extract the first loading/unloading cycle under various working conditions, and plot them together in Figure 5. For the first loading process, the accessible pore volume is the same for both the degassed and undegassed system. Although with different amount of residual gas in nanopores, there is no big difference for the first intrusion process at a certain contrast working condition because of the strong compressibility of gaseous phase. However, the disparate degrees of outflow phenomenon of systems with different gas amount prove that residual gas plays quite an important role in liquid outflow.

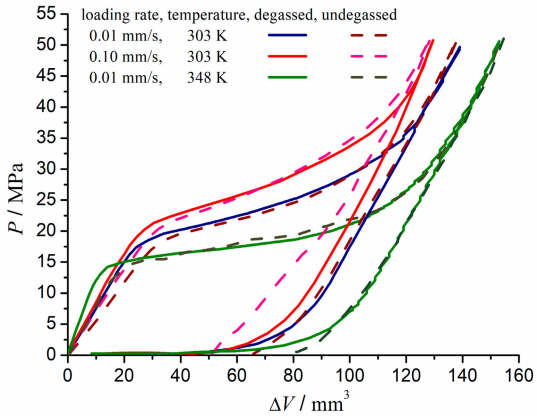

Figure 5. Comparision of the first loading/unloading cycle of undegassed and degassed glycerol/zeolite system (loading rate 0.01 mm/s and 0.10 mm/s; system temperature 303 K).

Define infiltration percentage as $\Delta V_{in}{}^{i}/\Delta V_{in}{}^{1}$ and defiltration percentage as $\Delta V_{de}{}^{i}/\Delta V_{in}{}^{1}$, where $\Delta V_{in}{}^{i}$ is the inflow volume of liquid during the ith intrusion process, and $\Delta V_{de}{}^{i}$ is the outflow volume of liquid after the ith loading/unloading cycle. During the first loading/unloading process, not the entire nanochannel will be filled with glycerol molecules, yet part of the glycerol molecules is trapped in the nanopores and could not flow out of the channels freely after the first cycle. Defects may be produced upon intrusion-extrusion cycles, by breaking Si-O-Si bonds into Si-OH (silanol) groups [21,33]. The incomplete outflow of the 1st cycle is partly due to trapped glycerol molecules and partly due to inelastic deformation of the system [18]. Assuming the infiltration volume of the first intrusion process $\Delta V_{in}{}^{1}$ as the maximum accessible infiltration volume, $\Delta V_{in}{}^{1}$ is taken as the baseline of measurement.

The infiltration and defiltration percentages of 10 loading/unloading cycles are portrayed in Figure 6. Both the infiltration and defiltration percentages of a degassed system are larger than that

of an undegassed system under a certain contrast working condition. As the difference between the degassed and undegassed system mainly ascribes to the amount of residual gas inside nanopores, it can be concluded that certain amount of residual gas helps liquid to flow out of nanopores, in turn to elevate the system's reversibility. When comparing the infiltration and defiltration percentage, more glycerol molecules tend to flow in and out of the nanochannels under higher loading rate, and at a lifted system temperature.

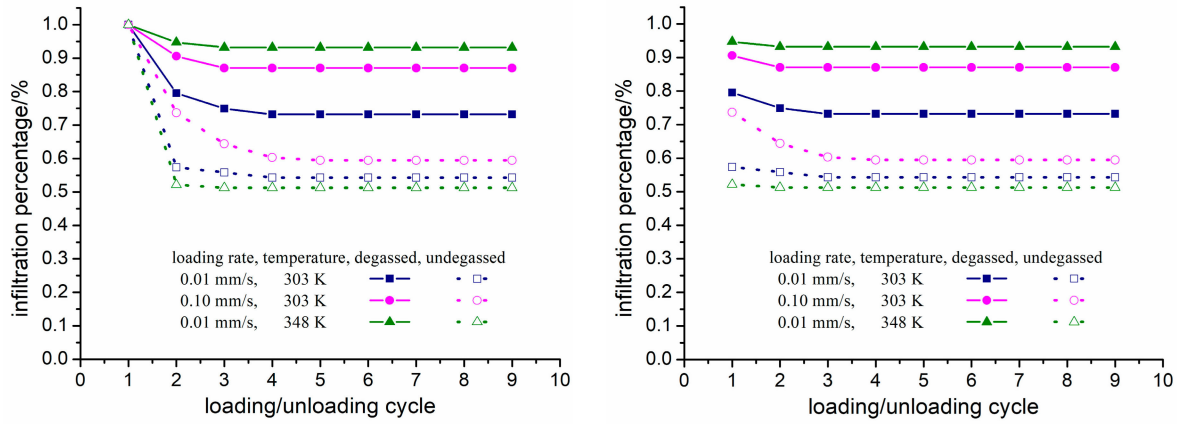

(**a**) infiltration percentage (**b**) defiltration percentage

Figure 6. Comparison of the infiltration and defiltration percentage of undegassed and degassed glycerol/zeolite system (loading rate 0.01 mm/s and 0.10 mm/s; system temperature 303 K and 348 K).

4. Discussion

When considering the different amounts of residual gas inside the system, the above phenomenon is proof of understanding the gas behavior under finite circumstances. In general, the gas in a liquid/nanoporous system can be divided into three categories: small bubbles standing in the mixture, the gas dissolved in the liquid, and the gas trapped in pores. For the undegassed condition, although the mixture are stood in atmosphere for 12 h during pretreatment, small bubbles that were introduced in the process of mixing glycerol and zeolite powder would not surface up spontaneously, as well as the gas dissolved and the gas trapped in pores. Therefore, the three categories of gas mentioned above are all included in the undegassed system. For the degassed mixture, as has been placed in vacuum for 12 h, the small bubbles dispersing in the mixture, together with the gas dissolved in the liquid as well, could be excluded. As a consequence, only the gas residual in the nanopores could not be eliminated during degassing pretreatment. To note that after pretreatment and before sealing, when the system is taken out of the vacuum condition, air would dissolved in liquid under atmospheric pressure. Assuming that in both degassed and undegassed cases, the amount of dissolved gas in the liquid are the same and equal to the solubility of air under atmospheric pressure. Therefore, the comparative differences between the above two working conditions are very obvious: there are small bubbles in the undegassed system (referring to Figure 2a), while none in the degassed system (referring to Figure 2b).

During intrusion and extrusion, the analyzed three categories of residual gas play different roles, which mainly depend on where the gas is trapped and how easily it dissolves in the liquid phase. According to Qiao's study, gas molecules tend to form clusters in nanochannels less than a few nanometers, which triggers liquid defiltration at a reduced pressure [25]. Since a molecular-sized nanoscale confinement arranges the gas and the water molecules into a single-file chain inside molecular-sized nanochannels [27,34], the radical confinement therefore provides a high resistance for molecular site exchanges [26]. Thus, the residual gas in nanopores under either undegassed or degassed systems helps to trigger the glycerol outflow. For a system spreading with small bubbles, although the gas solubility would increase with the increasing pressure, nevertheless, the undissolved gaseous phase would inevitably be pressed into the nanochannel during loading process, to form

a long or short section of gas cluster in the nanochannel. As the liquid is abundant in the testing systems, there is always liquid entering the channel. A cartoon depicting the status of gas-liquid in a nanochannel in the current system is given in Figure 7. Firstly, on the inside of the nanochannel, there is always a gas cluster consisting of the gas molecules that exists in nanopores originally. In a degassed system, a liquid column/chain fills the rest of the nanochannel until the open end, as depicted in Figure 7a. In an undegassed system, liquid column and gas cluster or gas molecule exist alternately with each other, as depicted in Figure 7b. In a hydrophobic system, the repelling force of the rigid wall to liquid is one of the most important driving forces for outflow during unloading. For instance, water in the hydrophobic zeolite behaves as a nanodroplet trying to close its hydrogen bonds onto itself, with a few short-lived dangling OH groups [35]. However, there is no such repelling force between the rigid wall and gas molecules. The inserted gas molecule interrupts the continuity of liquid chain, and the attractive intermolecular forces between liquid–liquid molecules is replaced by the repulsive force between the liquid and the gas molecules. Due to the lack of repelling force from the rigid wall and the insert of the repulsive force between liquid and gas molecules, the driving force for outflow decreases. Thus, the liquid phase tends to be trapped inside the nanochannel permanently. The trapped state of the nonwetting liquid appears as a result of a thermodynamic equilibrium among the interaction of the neighboring liquid-gas clusters and the liquid-solid interface.

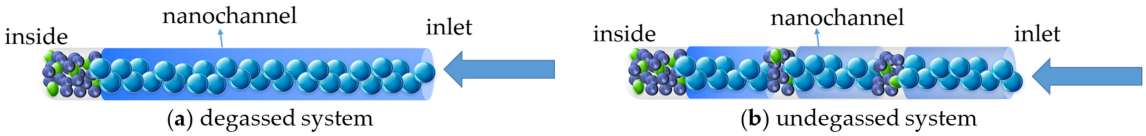

Figure 7. Cartoon of status of gas liquid in a nanochannel of degassed and undegassed systems. (gas cluster, liquid colum/chain.

In the undegassed system, the alternative distribution of the liquid column/chain and gas cluster/molecule is anisotropic and energetically unfavorable or unstable. The system stability is especially poor for the undegassed system under a higher loading rate (0.1 mm/s) and system temperature (348 K), as shown in Figure 4c,e. The fluctuations of the P-ΔV curves are probably caused by the uncompleted dissolution of small bubbles with a fast increased pressure under a high loading rate. The alternative distribution of the liquid column and the gas cluster is more likely to be formed in a nanochannel rather than a liquid column with gas molecule inserted distribution. Besides, this distribution is more unfavorable and energetically unstable. Through molecular thermal motion, gas, and liquid molecules adjacent will keep colliding with each other with high velocity and frequency in a random way, and hence, a gradual gas-liquid molecular site exchange can occur, despite in a much slower way than the diffusion process in the bulk phase in the sense of probability statistics. The higher the system temperature, the more furiously molecules collide each other, and the less stable the system is. In relatively large pores, gas channeling may also occur. These could be factors causing the fluctuation of P-ΔV curves in Figure 4e when the system temperature is 348 K.

To sum up, the influence of gas on a liquid/nanoporous system is mainly on the liquid outflow. On one hand, the originally existing gas in the nanochannel is compressed into a gas cluster, which will promote the liquid outflow during unloading. On the other hand, the excessively dissolved gas may break the continuity of the liquid molecular chain in the nanochannel and then the driving force for liquid outflow is reduced correspondingly, which in turn reduces the system's reversibility. Moreover, the increase of the amount of gas in the system will lead to instability if the excess small bubbles are not dissolved in time, especially under working conditions of a high loading rate or high system temperature.

5. Conclusions

In this study, a series of comparative experiment are carried out on a degassed glycerol/ZSM-5 zeolite system and an undegassed glycerol/ZSM-5 zeolite system. The effects of degassing on the stability and reversibility of glycerol/ZSM-5 zeolite system are studied by comparing the P-ΔV characteristics of different systems by varying the amount of residual gas, the loading rate, and the system temperature. Results show that it is impossible and unnecessary to fully eliminate the residual air in the nanopores by routine vacuum degassing pretreatment. Adequate residual air in nanopores, which is around 0.9014 nm^{-3} per unit specific pore volume air in the current study, is beneficial to elevate the system's reversibility. However, the vacuum degassing treatment is necessary to obtain a more reversible and stable energy absorption system. The originally existing air in nanopores is necessary to help the liquid outflow, nevertheless, excessively dissolved gas may reduce the driving force on liquid outflow by breaking the continuity of the liquid molecular chain in the nanochannel, let alone small bubbles, which are labile factor for the system's steady use. This work sheds some light on the effect of the residual amount of gas on the liquid/nanoporous material system and it gives us some guidance on the pretreatment of the liquid/nanoporous material mixture before encapsulating.

Author Contributions: Conceptualization, Y.Z., Q.Z. and X.C.; Methodology, Y.Z. and R.L.; Validation, Y.Z.; Formal Analysis, Y.Z. and R.L.; Resources, Q.Z. and Y.D.; Writing—Original Draft Preparation, Y.Z.; Writing—Review & Editing, R.L. and Y.D.; Supervision, Q.Z. and X.C. Funding Acquisition, Q.Z., Y.Z. and Y.D.

Funding: This research was funded by [Natural Science Foundation of Shaanxi Province of China] grant number [2017JQ5108], [Special Scientific Research Plan of Shaanxi Province Education Department] grant number [17JK0594], [National Science and Technology Major Project of the Ministry of Science and Technology of China] grant number [2016ZX05017-006-HZ03], [Ministry of Industry and Information Technology Support Project for High-Tech Ships] and [the Fundamental Research Funds for the Central Universities in Xi'an Jiaotong University].

Conflicts of Interest: The authors declare no conflict of interest. The funders had no role in the design of the study; in the collection, analyses, or interpretation of data; in the writing of the manuscript, and in the decision to publish the results.

References

1. Eroshenko, V.; Regis, R.; Soulard, M.; Patarin, J. Energetics: A new field of applications for hydrophobic zeolites. *J. Am. Chem. Soc.* **2001**, *123*, 8129–8130. [CrossRef] [PubMed]
2. Chen, X.; Qiao, Y. Science and prospects of using nanoporous materials for energy absorption. In *Life-Cycle Analysis for New Energy Conversion and Storage Systems*; Fthenakis, V., Dillon, A., Savage, N., Eds.; Cambridge University Press: Cambridge, MA, USA, 2008; Volume 1041, pp. 95–105.
3. Zhao, J.; Qiao, Y.; Culligan, P.J.; Chen, X. Confined liquid flow in nanotube: A numerical study and implications for energy absorption. *J. Comput. Theor. Nanosci.* **2009**, *7*, 379–387. [CrossRef]
4. Cao, G. Working mechanism of nanoporous energy absorption system under high speed loading. *J. Phys. Chem. C* **2012**, *116*, 8278–8286. [CrossRef]
5. Sun, Y.; Xu, J.; Li, Y.B.; Liu, B.; Wang, Y.; Liu, C.; Chen, X. Experimental study on energy dissipation characteristics of ZSM-5 zeolite/water system. *Adv. Eng. Mater.* **2013**, *15*, 740–746. [CrossRef]
6. Khay, I.; Chaplais, G.; Nouali, H.; Ortiz, G.; Marichal, C.; Patarin, J. Assessment of the energetic performances of various zifs with sod or rho topology using high pressure water intrusion-extrusion experiments. *Dalton Trans.* **2016**, *45*, 4392–4400. [CrossRef] [PubMed]
7. Sun, Y.; Guo, Z.; Xu, J.; Xu, X.; Liu, C.; Li, Y. A candidate of mechanical energy mitigation system: Dynamic and quasi-static behaviors and mechanisms of zeolite β/water system. *Mater. Des.* **2015**, *66*, 545–551. [CrossRef]
8. Li, M.; Lu, W. Liquid marble: A novel liquid nanofoam structure for energy absorption. *AIP Adv.* **2017**, *7*, 055312. [CrossRef]
9. Chen, X.; Surani, F.B.; Kong, X.; Punyamurtula, V.K. Energy absorption performance of steel tubes enhanced by a nanoporous material functionalized liquid. *Appl. Phys. Lett.* **2006**, *89*, 241918. [CrossRef]
10. Liu, Y.; Schaedler, T.A.; Jacobsen, A.J.; Lu, W.; Qiao, Y.; Chen, X. Quasi-static crush behavior of hollow microtruss filled with nmf liquid. *Compos. Struct.* **2014**, *115*, 29–40. [CrossRef]

11. Sun, Y.; Li, Y.; Zhao, C.; Wang, M.; Lu, W.; Qiao, Y. Crushing of circular steel tubes filled with nanoporous-materials-functionalized liquid. *Int. J. Damage Mech.* **2018**, *27*, 439–450. [CrossRef]
12. Sun, Y.; Xu, X.; Xu, C.; Qiao, Y.; Li, Y. Elastomeric cellular structure enhanced by compressible liquid filler. *Sci. Rep.* **2016**, *6*, 26694. [CrossRef] [PubMed]
13. Xu, J.; Hu, R.; Chen, X.; Hu, D. Impact protection behavior of a mordenite zeolite system. *Eur. Phys. J. Spec. Top.* **2016**, *225*, 363–373. [CrossRef]
14. Li, M.; Lu, W. Adaptive liquid flow behavior in 3d nanopores. *Phys. Chem. Chem. Phys.* **2017**, *19*, 17167–17172. [CrossRef] [PubMed]
15. Surani, F.B.; Kong, X.; Panchal, D.B.; Qiao, Y. Energy absorption of a nanoporous system subjected to dynamic loadings. *Appl. Phys. Lett.* **2005**, *87*, 163111. [CrossRef]
16. Han, A.; Punyamurtula, V.K.; Qiao, Y. Heat generation associated with pressure-induced infiltration in a nanoporous silica gel. *J. Mater. Res.* **2008**, *23*, 1902–1906. [CrossRef]
17. Lefevre, B.; Saugey, A.; Barrat, J.L.; Bocquet, L.; Charlaix, E.; Gobin, P.F.; Vigier, G. Intrusion and extrusion of water in hydrophobic mesopores. *J. Chem. Phys.* **2004**, *120*, 4927. [CrossRef] [PubMed]
18. Zhang, Y.; Li, N.; Luo, R.; Zhang, Y.; Zhou, Q.; Chen, X. Experimental study on thermal effect on infiltration mechanisms of glycerol into ZSM-5 zeolite under cyclic loadings. *J. Phys. D Appl. Phys.* **2016**, *49*, 025303. [CrossRef]
19. Yu, M.C.; Gao, X.; Chen, Q. Nonlinear frequency response analysis and jump avoidance design of molecular spring isolator. *J. Mech.* **2016**, *32*, 527–538. [CrossRef]
20. Borman, V.D.; Belogorlov, A.A.; Byrkin, V.A.; Tronin, V.N.; Troyan, V.I. Stability of a nonwetting liquid in a nanoporous medium. *Phys. Scr.* **2014**, *89*. [CrossRef]
21. Watt-Smith, M.J.; Rigby, S.P.; Chudek, J.A.; Fletcher, R. Simulation of nonwetting phase entrapment within porous media using magnetic resonance imaging. *Langmuir* **2006**, *22*, 5180–5188. [CrossRef] [PubMed]
22. Kong, X.; Qiao, Y. Improvement of recoverability of a nanoporous energy absorption system by using chemical admixture. *Appl. Phys. Lett.* **2005**, *86*, 151919. [CrossRef]
23. Sun, Y.; Lu, W.; Li, Y. A defiltration control method of pressurized liquid in zeolite ZSM-5 by silanol introduction. *Appl. Phys. Lett.* **2014**, *105*, 121609. [CrossRef]
24. Kong, X.; Qiao, Y. Thermal effect on pressure induced infiltration of a nanoporous system. *Phil. Mag. Lett.* **2005**, *85*, 331–337. [CrossRef]
25. Qiao, Y.; Cao, G.; Chen, X. Effects of gas molecules on nanofluidic behaviors. *J. Am. Chem. Soc.* **2007**, *129*, 2355–2359. [CrossRef] [PubMed]
26. Sun, Y.; Li, P.; Yu, Q.; Li, Y. Time-dependent gas-liquid interaction in molecular-sized nanopores. *Sci. Rep.* **2014**, *4*, 6547. [CrossRef] [PubMed]
27. Hummer, G.; Rasaiah, J.C.; Noworyta, J.P. Water conduction through the hydrophobic channel of a carbon nanotube. *Nature* **2001**, *414*, 188–190. [CrossRef] [PubMed]
28. Majumder, M.; Chopra, N.; Andrews, R.; Hinds, B.J. Nanoscale hydrodynamics: Enhanced flow in carbon nanotubes. *Nature* **2005**, *438*, 44. [CrossRef] [PubMed]
29. Holt, J.K.; Park, H.G.; Wang, Y.; Stadermann, M.; Artyukhin, A.B.; Grigoropoulos, C.P.; Noy, A.; Bakajin, O. Fast mass transport through sub-2-nanometer carbon nanotubes. *Science* **2006**, *312*, 1034. [CrossRef] [PubMed]
30. Sholl, D.S.; Johnson, J.K. Making high-flux membranes with carbon nanotubes. *Science* **2006**, *312*, 1003–1004. [CrossRef] [PubMed]
31. Chen, X.; Cao, G.; Han, A.; Punyamurtula, V.K.; Liu, L.; Culligan, P.J.; Kim, T.; Qiao, Y. Nanoscale fluid transport: Size and rate effects. *Nano Lett.* **2008**, *8*, 2988. [CrossRef] [PubMed]
32. Bushuev, Y.G.; Sastre, G.; Juliánortiz, J.V.D.; Gálvez, J. Water-hydrophobic zeolite systems. *J. Phys. Chem. C* **2012**, *116*, 24916–24929. [CrossRef]
33. Kumzerov, Y.A.; Nabereznov, A.A.; Vakhrushev, S.B.; Savenko, B.N. Freezing and melting of mercury in porous glass. *Phys. Rev. B Condens. Matter* **1995**, *52*, 4772–4774. [CrossRef] [PubMed]

34. John A, T. Water flow in carbon nanotubes: Transition to subcontinuum transport. *Phys. Rev. Lett.* **2009**, *102*, 184502.
35. Rigby, S.P.; Edler, K.J. The influence of mercury contact angle, surface tension, and retraction mechanism on the interpretation of mercury porosimetry data. *J. Colloid Interface Sci.* **2002**, *250*, 175–190. [CrossRef] [PubMed]